Delayed Wound Closure and Phenotypic Changes in Corneal Epithelium of the Spontaneously Diabetic Goto-Kakizaki Rat

Makiko Wakuta,[1] *Naoyuki Morishige,*[1] *Tai-ichiro Chikama,*[1] *Keisuke Seki,*[2] *Takashi Nagano,*[3] *and Teruo Nishida*[1]

Purpose. To characterize wound closure and phenotypic changes in the corneal epithelium of the Goto-Kakizaki (GK) rat, a spontaneous model of type 2 diabetes.

Methods. Corneal wound healing was monitored by fluorescein staining after epithelial debridement. Tear secretion was measured with the Schirmer test, and corneal sensation was evaluated with an esthesiometer in 13- to 15-week-old GK and Wistar (control) rats. The distributions of cytokeratin 12 (K12), K14, and connexin43 in the corneal epithelium were examined by immunohistofluorescence analysis. The proliferation capacity of epithelial cells in the intact cornea and during wound healing was evaluated by immunostaining for Ki-67.

Results. Tear secretion, corneal sensation, and corneal epithelial wound closure rate were all decreased in GK rats compared with those in Wistar rats. Whereas connexin43, K14, and Ki-67 were all restricted to the single layer of basal cells in the corneal epithelium of Wistar rats, they were detected in the two layers of cells closest to the basement membrane in that of GK rats. The frequency of Ki-67–positive cells in the intact corneal epithelium was greater in GK rats than in Wistar rats, and it was increased to a greater extent in the peripheral cornea of GK rats than in that of Wistar rats during wound healing.

Conclusions. Spontaneously diabetic GK rats manifest characteristics similar to those of diabetic keratopathy in humans, including delayed wound closure, and they exhibit phenotypic changes in corneal epithelial cells. (*Invest Ophthalmol Vis Sci.* 2007;48:590–596) DOI:10.1167/iovs.05-1168

Complications of diabetes mellitus that affect the eye represent an increasing threat to sight because of the increasing prevalence of this condition worldwide.[1] In addition to diabetic retinopathy, various types of corneal epithelial disorder are relatively common in persons with diabetes.[2,3] Although the cornea is transparent and appears normal in patients with diabetic keratopathy in the absence of corneal injury, damage to the corneal epithelium reveals that epithelial wound healing and the re-formation of the normal stratified structure of the epithelium are delayed.[4,5] Abnormalities of the basement membrane of the corneal epithelium, including thickening,[6–8] degeneration,[9–12] increased nonenzymatic glycation of protein components,[13] and deposition of advanced glycation end products,[14] have been detected in diabetic humans and animal models of diabetes. Moreover, the functions of corneal epithelial cells are also altered in the diabetic state.[15–18] The underlying pathology of diabetic keratopathy is thus characterized by abnormalities of the epithelial basement membrane and epithelial cells.

The normal corneal epithelium is a nonkeratinized, stratified, squamous epithelium that consists of basal cells, wing cells, and superficial cells. A single layer of basal cells sits on the basement membrane. These cells mature consecutively into wing cells and superficial cells. The normal structure and functions of the corneal epithelium are maintained by a constant turnover of cells that is the result of an appropriate balance among the proliferation, differentiation, and maturation of epithelial cells.[19] In the central cornea, only the basal cells are able to proliferate, and this ability is lost in association with further maturation. Corneal epithelial cells express cytokeratin 12 (K12).[20] Cytokeratin 14 (K14), a marker of basal cells in stratified squamous epithelia, is expressed only in the basal cell layer of the corneal epithelium.[21] Connexin43 (Cx43), the major protein component of gap junctions, is also expressed only in the basal cell layer of the corneal epithelium.[22,23] The expression of K14 and Cx43 is thus downregulated as the basal cells of the corneal epithelium mature. The expression pattern of Cx43 changes during corneal epithelial wound healing but is restored as healing is completed.[24,25] Components of the basement membrane, including laminin, fibronectin, tenascin, and type IV collagen, also play important roles in maintaining the corneal epithelium and in wound healing.[26–29]

The Goto-Kakizaki (GK) rat is a spontaneous model of type 2 diabetes that was produced as a result of selective breeding over many generations of nondiabetic Wistar rats with glucose intolerance.[30,31] GK rats develop mild hyperglycemia in the absence of obesity and hyperlipidemia. Pathologic changes in various organs and tissues, including the kidneys[32,33] and nerves,[34] of GK rats resemble those apparent in patients with diabetes. The deposition of extracellular matrix proteins such as type IV collagen has thus been shown to be increased in the kidneys of GK rats.[32,33] Furthermore, GK rats manifest various abnormalities of the eye, including decreased retinal circulation,[35] increased retinal production of nitric oxide,[36] upregulation of vascular endothelial growth factor,[37] and increased abundance of O-GlcNAc–modified proteins in the cornea.[38]

To investigate the underlying mechanisms of corneal epithelial disorders associated with diabetes mellitus, with the use of immunohistochemical techniques we have now characterized the expression of K12, K14, Cx43, and Ki-67 (a marker of cell proliferation capacity) in the intact or wounded cornea of diabetic GK rats in comparison with nondiabetic Wistar (WKY) rats.

From the Departments of [1]Ophthalmology and [2]Ocular Pathophysiology, Yamaguchi University Graduate School of Medicine, Yamaguchi, Japan; and the [3]Research and Development Center, Santen Pharmaceutical Co. Ltd., Nara, Japan.

Submitted for publication September 1, 2005; revised February 7 and July 18, 2006; accepted December 18, 2006.

Disclosure: **M. Wakuta**, None; **N. Morishige**, None; **T. Chikama**, None; **K. Seki**, None; **T. Nagano**, None; **T. Nishida**, None

The publication costs of this article were defrayed in part by page charge payment. This article must therefore be marked "*advertisement*" in accordance with 18 U.S.C. §1734 solely to indicate this fact.

Corresponding author: Makiko Wakuta, Department of Ophthalmology, Yamaguchi University Graduate School of Medicine, 1-1-1 Minami-Kogushi, Ube City, Yamaguchi 755-8505, Japan; wakumaki@sk2.so-net.ne.jp.

METHODS

Animals

Male GK rats and normal male Wistar rats were obtained from Charles River Japan (Yokohama, Japan). The animals were allowed free access to laboratory chow and water and were studied at 13 to 15 weeks of age. The study was performed in accordance with the ARVO Statement for the Use of Animals in Ophthalmic and Vision Research and was approved by the animal ethics committee of Yamaguchi University Graduate School of Medicine.

Measurement of Tear Secretion and Corneal Sensation

Tear secretion in rats was determined with a modified Schirmer test. The test was performed without topical anesthesia. Schirmer strips (Showa Yakuhin Kako, Tokyo, Japan), cut to a length of 17 mm and a width of 1 mm, were inserted behind the lower eyelid near the medial canthus for 1 minute. The wet length of the strip was then measured. Corneal sensation of rats was measured with a Cochet-Bonnet esthesiometer. Initially, the nylon filament was fully extended to 60 mm. Objective blinking was considered a positive response. If a positive response was not detected, the fiber length was shortened 5 mm at a time, and the procedure was repeated until such a response was obtained. The test was repeated three times, and the average of the three measurements was determined.

Corneal Epithelial Wound Healing

Rats were anesthetized by intraperitoneal injection of sodium pentobarbital (30 mg/kg body weight) and the application of 0.4% oxybuprocain hydrochloride to each eye. The entire epithelium of each cornea was then removed with a blunt blade. The epithelial defect was stained with 1% fluorescein and photographed at 10, 24, 34, 48, 58, 72, 82, and 96 hours after debridement. The area of the epithelial defect was measured on the photographs with a computer-assisted image analyzer. Changes in the defect area were plotted graphically, and the healing rate was calculated by linear regression from the data obtained between 10 and 48 hours after debridement.

Immunohistochemistry

Rats were killed by intraperitoneal injection of an overdose of sodium pentobarbital (Kyoritsu Seiyaku, Tokyo, Japan) before or 36 or 72 hours after total corneal epithelial debridement. Both eyeballs were enucleated, rinsed with phosphate-buffered saline (PBS), immersed in OCT compound (Sakura Finechemical, Tokyo, Japan), frozen with liquid nitrogen, and stored at −80°C. Sections of the eyeball were cut at a thickness of 6 μm with a cryostat (Microm HM505E; Richard-Allan Scientific, Kalamazoo, MI), and four sections were mounted on each glass slide. The sections were allowed to dry in air at room temperature and were then fixed in absolute acetone for 10 minutes. After washing with PBS, the sections were incubated for 20 minutes in solution (Block Ace; Dainippon Seiyaku, Osaka, Japan) and were then processed for immunohistochemistry.

Antibodies and other reagents used for immunostaining are listed, together with their incubation times and dilutions, in Table 1. All incubations were performed at room temperature unless indicated otherwise. Sections for immunofluorescence analysis were mounted (SlowFade Light Antifade Kit; Molecular Probes, Eugene, OR) in the presence of 4′,6-diamidino-2-phenylindole (DAPI), observed with an epifluorescence microscope (Axioscop2; Carl Zeiss, München-Hallbergmoos, Germany) and were photographed with a digital camera system (Axiocam; Carl Zeiss). The same fields were photographed under Nomarski optics, and the Nomarski and immunofluorescence images were overlaid. Sections processed for the horseradish peroxidase (HRP) reaction were developed with diaminobenzidine solution (DAB Kit; Zymed, South San Francisco, CA) for 5 minutes and then incubated with the enhanced solution for an additional 5 minutes. They were then fixed with 4% formaldehyde for 1 minute, stained with hematoxylin (to reveal nuclei), dehydrated with a graded series of alcohol solutions, cleared with xylene, and mounted with permanent mounting medium. The sections were also observed with a microscope (Axioscop2; Carl Zeiss) and photographed with a digital camera system (Axiocam; Carl Zeiss).

For double staining of K12, K14, or Cx43 with laminin, the sections were incubated with primary antibodies to K12, K14, or Cx43, washed three times with PBS, and incubated with fluorescent dye (Alexa Fluor 488; Molecular Probes)–conjugated secondary antibodies to rabbit or mouse immunoglobulin G (IgG). The sections were then washed with PBS, incubated with biotinylated rabbit antibodies to laminin, washed again with PBS, and incubated with fluorescent dye (Alexa Fluor 555; Molecular Probes)–conjugated streptavidin. Double staining of Cx43 and K14 was performed similarly but with the use of mouse antibodies to K14 and conjugated (Alexa Fluor 555; Molecular Probes) rabbit antibodies to mouse IgG.

For examination of cell proliferation capacity in the intact or wounded cornea, four eyes of four Wistar rats and four eyes of four GK rats were processed for immunohistochemical staining of Ki-67. The central portion of each cornea was serially sectioned, and four sections of each eye were examined. Frozen sections prepared and fixed as described above and were stained with mouse antibodies to Ki-67,

TABLE 1. Antibodies, Other Reagents, and Incubation Conditions Used for Immunohistochemistry

Antibodies and Other Reagents	Supplier	Catalog No.	Dilution	Incubation Time (min)
Rabbit polyclonal anti-C×43	Chemicon	ab1728	1:100	60
Mouse monoclonal anti-K14	YLE	MCC703	1:20	90
Rabbit polyclonal anti-mouse K12	W. W. Kao, University of Cincinnati; S. Saika, Wakayama Medical University, Japan		1:100	60
Biotinylated rabbit polyclonal anti-human laminin	Abcam	ab6571	1:500	30
Mouse monoclonal anti-Ki-67	DAKO	M7248	1:25	45
Alexa Fluor 488–conjugated goat polyclonal anti-rabbit IgG	Molecular Probes	A-11008	1:1000	30
Alexa Fluor 488–conjugated rabbit polyclonal anti-mouse IgG	Molecular Probes	A-11001	1:1000	30
Alexa Fluor 555–conjugated streptavidin	Molecular Probes	S32355	1:1000	30
Alexa Fluor 555–conjugated rabbit polyclonal anti-mouse IgG	Molecular Probes	A-21424	1:1000	30
Biotinylated rabbit polyclonal anti-mouse IgG	DAKO	E0464	1:300	30
HRP-conjugated streptavidin	DAKO	P0397	1:300	30

biotinylated rabbit antibodies to mouse IgG, and HRP-conjugated streptavidin. The number of Ki-67–positive cells and the length of the basement membrane from limbus to limbus were measured for the intact cornea and for the wounded cornea at 72 hours after debridement, and the number of Ki-67–positive cells per 100 μm basement membrane was calculated. Given that the epithelial wounds had not closed at 36 hours after debridement, the density of Ki-67–positive cells was calculated for the one third of the total length of the basement membrane measured from the limbus.

Transmission Electron Microscopy

The cornea was dissected from the enucleated eyeball and fixed for 2 hours at 4°C in 0.1 M phosphate buffer (pH 7.4) containing 2% formaldehyde and 2% glutaraldehyde. After washing with 0.1 M phosphate buffer, the tissue was exposed for 2 hours at 4°C to 1% osmium tetroxide, washed with distilled water, incubated for 3 hours at room temperature with saturated uranyl acetate solution, dehydrated in a graded series of alcohol solutions, and embedded in Epon epoxy resin. Ultrathin sections were cut with a microtome (Ultracut E; Leica Microsystems, Wetzlar, Germany) and stained with uranyl acetate and lead citrate. They were then observed with an electron microscope (H-7500; Hitachi, Yokohama, Japan) and photographed. For immunoelectron microscopy of Cx43, tissue was incubated consecutively overnight at 4°C with the primary antibodies (1:100 dilution in PBS containing 0.1% Triton X-100) listed in Table 1, for 2 hours at room temperature with HRP-conjugated goat antibodies to rabbit IgG (1:200 dilution; Envision+, DAKO, Carpinteria, CA), and for 5 minutes at room temperature with diaminobenzidine before exposure to osmium tetroxide.

Statistical Analysis

Quantitative data are presented as mean ± SD and were compared by the unpaired Student's *t* test or the Wilcoxon test, as indicated. $P < 0.05$ was considered statistically significant.

Results

Clinical Characteristics of GK Rats

The body mass of GK rats at 13 to 15 weeks of age was significantly lower than that of age-matched Wistar control rats (Table 2). Blood glucose concentrations of GK rats in the randomly fed state were significantly higher than of Wistar rats. Tear secretion and corneal sensation were significantly decreased in GK rats compared with those in Wistar rats.

Corneal Epithelial Wound Healing

We examined the pattern of corneal epithelial wound healing in GK rats. Immediately after corneal epithelial debridement, there was no significant difference in the area of the wound between Wistar and GK rats (25.71 ± 1.1 mm^2 and 25.41 ± 1.6 mm^2, respectively; $P = 0.61$, Student's *t* test). Closure of the corneal wound after epithelial debridement was completed in GK and Wistar rats (Fig. 1A). However, although the epithelial defect had healed almost completely by 48 hours in Wistar rats, it was still apparent at 72 hours in GK rats. Quantitative analysis revealed that the rate of wound healing was 0.611 ± 0.047 mm^2/h in Wistar rats and 0.509 ± 0.043 mm^2/h in GK rats ($P < 0.01$; Student's *t* test; Fig. 1B). Corneal epithelial wound healing was thus significantly delayed in GK rats compared with healing in Wistar rats.

Table 2. Clinical Characteristics of GK and Wistar Control Rats at 13 to 15 Weeks of Age

Characteristic	Wistar	GK	*P*
Body mass (g)	474 ± 31	347 ± 17	<0.01*
Blood glucose (mg/dL)	116 ± 11	259 ± 55	<0.01*
Tear secretion (mm/min)	10.2 ± 1.6	5.8 ± 1.8	<0.01*
Corneal sensation (g/mm^2)	0.4 ± 0.0	1.9 ± 1.1	<0.01†

Data are mean ± SD of values from five Wistar and six GK rats (10 and 12 eyes, respectively).

* Student's *t* test.

†Wilcoxon test (signed-rank).

Immunolocalization of K12, K14, and Cx43 in the Corneal Epithelium

We next performed immunofluorescence analysis to examine the localization of K12, K14, or Cx43 together with that of laminin in the corneal epithelium of GK rats. In GK and Wistar rats, K12 was detected in all corneal epithelial cells (Figs. 2A, 2B). In Wistar rats, K14 (Fig. 2C) and Cx43 (Fig. 2E) were expressed only in the single layer of basal epithelial cells associated with the basement membrane, as revealed by staining for laminin. However, in GK rats, K14 (Fig. 2D) and Cx43 (Fig. 2F) were apparent in the two layers of epithelial cells adjacent to the basement membrane.

To confirm the localization of K14 and Cx43 to this double layer of cells in the corneal epithelium of GK rats, we stained for K14 and Cx43 in the same sections (Fig. 3). Again, the two layers of cells at the base of the corneal epithelium were positive for K14 and Cx43 in GK rats (Figs. 3B, 3D), whereas only the single layer of basal cells associated with the basement membrane was positive for these two proteins in Wistar rats (Figs. 3A, 3C).

Transmission Electron Microscopy

Transmission electron microscopy revealed the corneal epithelium of Wistar rats as a nonkeratinized, stratified, squamous epithelium composed of basal, wing, and superficial cells. The single basal cell layer consisted of columnar cells, and the wing cells located superior to the basal cell layer exhibited a cell morphology that was spinous and had thin cytoplasmic processes. In contrast, in the corneal epithelium of GK rats, basal cells were cuboidal and were shorter than those in Wistar rats, and they formed a double layer below the wing cell layer. Basal cells were directly associated with the basement membrane in Wistar and GK rats, and hemidesmosomes were present on the basal surfaces of the cells in contact with the basement membrane. The basal lamina of GK rats, however, was thicker than that of Wistar rats. Basal cells and wing cells made contact with each other through interdigitations and desmosomes in both types of rat, but the wing cells of GK rats manifested fewer interdigitations than did those of Wistar rats. Tight junctions were observed between superficial cells in Wistar and GK rats (data not shown).

Immunoelectron Microscopy

Immunoelectron microscopic analysis of Cx43 expression confirmed Cx43 immunoreactivity only in the single layer of columnar basal cells in the corneal epithelium of Wistar rats. In GK rats, Cx43 immunoreactivity was observed not only between the cells associated with the basement membrane but also between the cuboidal cells located superior to them. Higher magnification images revealed that Cx43 immunoreactivity was associated with gap junctions in Wistar and GK rats (data not shown).

Epithelial Cell Proliferation

We next examined cell proliferation capacity in the corneal epithelia of GK and Wistar rats by staining for Ki-67. In Wistar rats, Ki-67–positive cells were detected only in the single layer

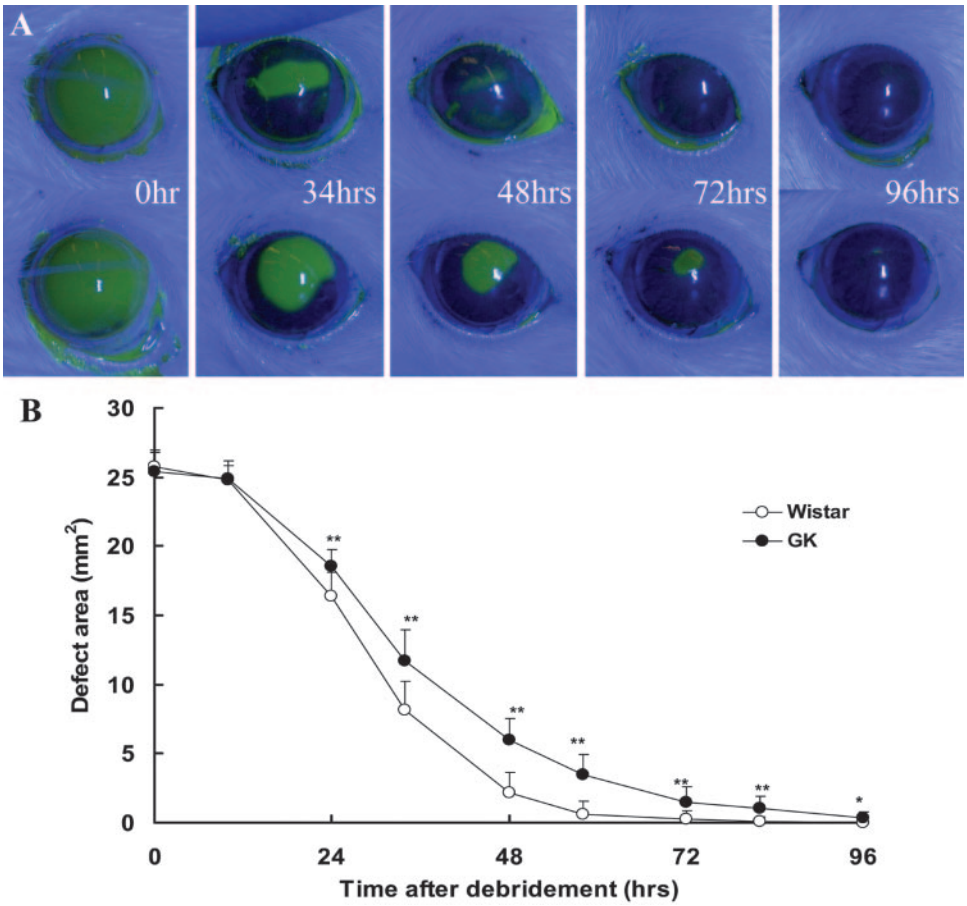

FIGURE 1. Corneal epithelial wound healing in GK and Wistar rats. (**A**) Fluorescein staining of corneal epithelial defects at the indicated times after epithelial debridement in Wistar (*upper panels*) and GK (*lower panels*) rats. (**B**) Quantitative analysis of the time course of corneal epithelial wound healing. Data are means ± SD of values from 10 (Wistar) or 12 (GK) eyes. $^{*}P < 0.05$ and $^{**}P < 0.01$ versus corresponding value for Wistar rats (Student's *t* test).

of basal cells associated with the basement membrane (Figs. 4A, 4C). In contrast, Ki-67–positive cells were apparent in the basal cell layer directly associated with the basement membrane and in the immediately superior cell layer of GK rats (Figs. 4B, 4D). Quantitative analysis revealed that the number of Ki-67–positive cells per 100-μm length of basement membrane was significantly higher in GK rats (1.40 ± 0.11 cells/100 μm) than in Wistar rats (1.00 ± 0.11 cells/100 μm; Fig. 4E).

Epithelial Cell Proliferation during Corneal Epithelial Wound Healing

Finally, we examined the proliferation capacity of epithelial cells in central and peripheral regions of the cornea during epithelial wound healing. The number of Ki-67–positive cells

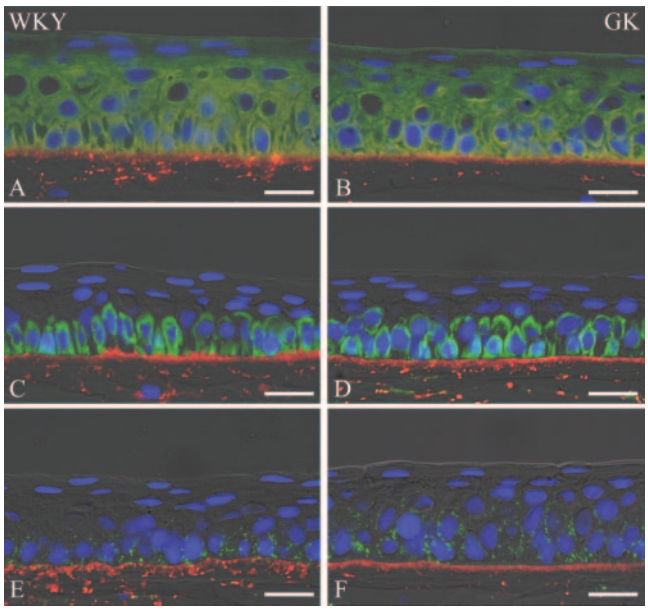

FIGURE 2. Immunolocalization of K12, K14, or Cx43 with laminin in the corneal epithelium of GK and Wistar rats. Corneal epithelia of Wistar (**A**, **C**, **E**) and GK (**B**, **D**, **F**) rats were immunostained for laminin (*red*) and K12 (**A**, **B**), K14 (**C**, **D**), or Cx43 (**E**, **F**) (*green*). Nuclei were stained with DAPI (*blue*). Scale bars, 20 μm.

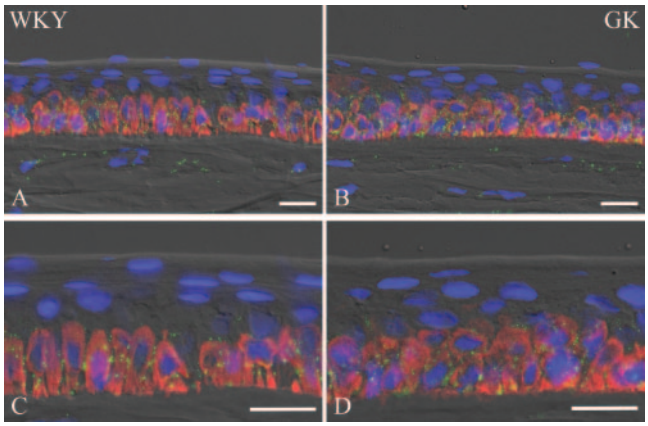

FIGURE 3. Immunolocalization of Cx43 and K14 in the corneal epithelia of GK and Wistar rats. Corneal epithelia of Wistar (**A**, **C**) and GK (**B**, **D**) rats were immunostained for Cx43 (*green*) and K14 (*red*). Nuclei were stained with DAPI (*blue*). (**A**) and (**B**) are shown at higher magnification in (**C**) and (**D**). Scale bars, 20 μm.

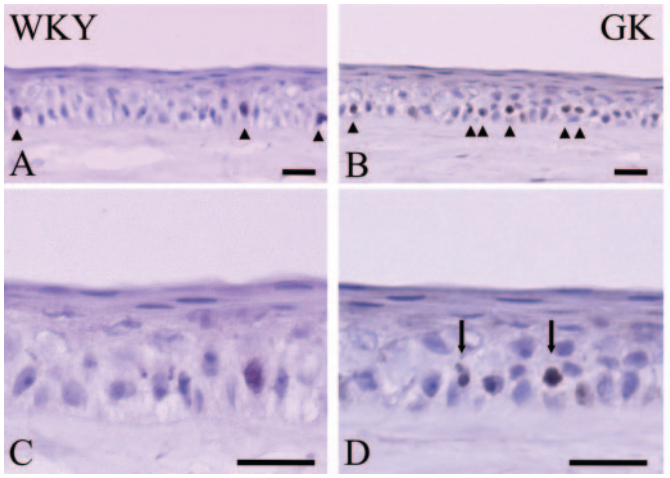

FIGURE 4. Cell proliferation capacity in the corneal epithelium of GK and Wistar rats. (**A–D**) Immunohistochemical analysis of the corneal epithelium of Wistar (**A**, **C**) and GK (**B**, **D**) rats with antibodies to Ki-67. The frequency of Ki-67–positive cells (*arrowheads*) was greater in GK rats (**B**) than in Wistar rats (**A**). Higher magnification images revealed that these cells were present in the basal cell layer of Wistar rats (**C**) but in both the basal layer and the suprabasal layer (*arrows*) of GK rats (**D**). Scale bars, 20 μm. (**E**) Quantitation of Ki-67–positive cells per 100-μm length of basement membrane. Data are mean ± SD ($n = 4$). $^*P < 0.01$ (Studen's t test).

in the central region of the intact cornea was greater for GK rats than for Wistar rats, and these cells were present in a double layer in GK rats (Figs. 5A, 5G). At 36 hours after epithelial debridement, Ki-67–positive cells were sparsely distributed in the region of the wound margin in both types of rat (Figs. 5B, 5H). At 72 hours after debridement, when the wound had closed in Wistar rats and had almost closed in GK rats and the multilayered structure of the epithelium had been restored, the number of Ki-67–positive cells was still reduced in both types of rat compared with that apparent in the corresponding intact cornea (Figs. 5C, 5I). However, the Ki-67–positive cells in GK rats were again present in a double layer.

The number of Ki-67–positive cells in the peripheral region of the intact cornea was also greater for GK rats than for Wistar rats, and again these cells were present in a double layer in GK rats (Figs. 5D, 5J). The number of Ki-67–positive cells in the peripheral region of the cornea of Wistar rats was increased 36 hours after epithelial debridement (Fig. 5E), with these cells forming a double layer in places, but it returned to normal by 72 hours (Fig. 5F). The number of Ki-67–positive cells in the peripheral region of the cornea of GK rats was also increased 36 hours after debridement (Fig. 5K), and it remained so at 72 hours (Fig. 5L). Immunostaining for Cx43 and K14 at 36 hours after epithelial debridement also revealed that the immunofluorescence-positive epithelial cells in the peripheral region of the cornea formed a continuous double layer in GK rats but an almost uniform single layer in Wistar rats (Figs. 5M, 5N).

In addition, we performed quantitative analysis of corneal epithelial cell proliferation during epithelial wound healing. The number of Ki-67–positive cells per 100-μm length basement membrane at 36 or 72 hours after debridement was significantly greater in GK rats than in Wistar rats (Fig. 6).

DISCUSSION

We have shown that tear secretion, corneal sensation, and corneal epithelial wound closure rate are all decreased in the GK rat, a spontaneous model of type 2 diabetes, compared with those in the nondiabetic Wistar rat. Immunoreactivity for Cx43, K14, and Ki-67 was also detected in the two layers of cells adjacent to the basement membrane in the corneal epithelium of GK rats, whereas only the single basal layer of cells was positive for these proteins in the corneal epithelium of control rats. Furthermore, we found that the proliferation capacity of corneal epithelial cells was increased in GK rats compared with that in Wistar rats. Our results thus demonstrate that the structure of the corneal epithelium and the proliferation capacity of corneal epithelial cells are abnormal in

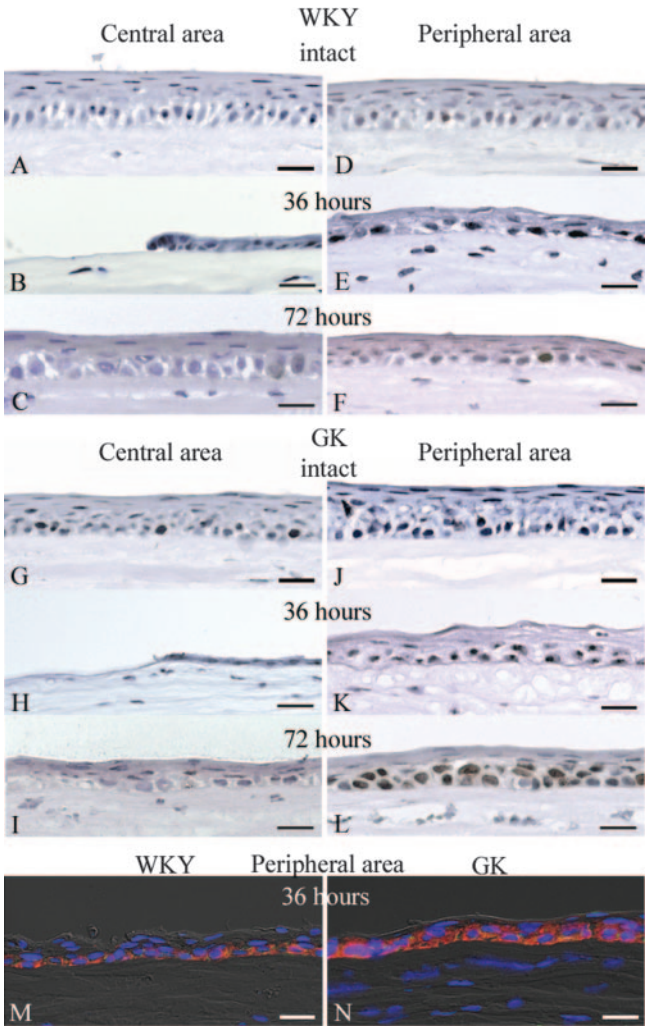

FIGURE 5. Immunolocalization of Ki-67, Cx43, and K14 in the peripheral or central regions of the cornea during wound healing in GK and Wistar rats. Central (**A–C**, **G–I**) and peripheral (**D–F**, **J–L**) regions of the corneal epithelia of Wistar (**A–F**) and GK (**G–L**) rats were immunostained for Ki-67 before (**A**, **D**, **G**, **J**) or 36 hours (**B**, **E**, **H**, **K**) or 72 hours (**C**, **F**, **I**, **L**) after epithelial debridement. Peripheral region of the corneal epithelium of Wistar (**M**) and GK (**N**) rats was immunostained for Cx43 (*green*) and K14 (*red*) 36 hours after epithelial debridement. Nuclei were also stained with DAPI (*blue*). Scale bars, 20 μm.

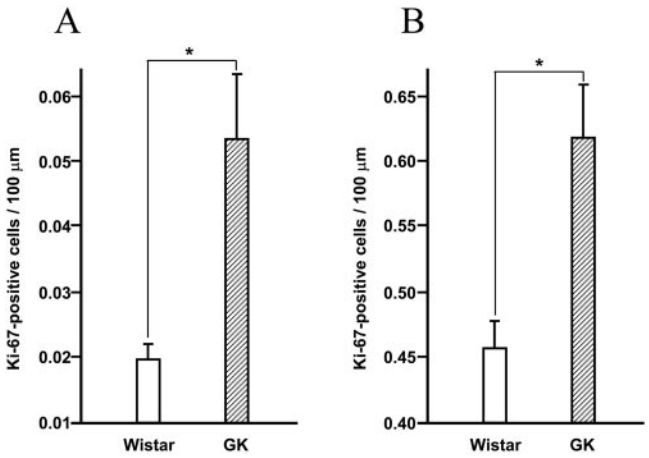

FIGURE 6. Quantitative analysis of Ki-67–positive epithelial cells per 100-μm length of basement membrane at 36 hours (**A**) and 72 hours (**B**) after corneal epithelial debridement in GK and Wistar rats. Data are mean ± SD ($n = 3$). $^*P < 0.05$ (Student's t test).

GK rats, with these abnormalities possibly contributing to the delay in corneal epithelial wound healing also apparent in these animals.

Immunostaining for Ki-67 indicated that the proliferation capacity of basal cells in the corneal epithelium of GK rats is greater than in Wistar rats. This difference was apparent in the intact cornea and during the healing of corneal epithelial wounds; during wound healing, it was more pronounced in the peripheral region of the cornea than at the wound margin in the central region. This increased proliferation capacity of epithelial cells in the cornea of GK rats was associated with a delay in the resurfacing of epithelial defects. Increased cell number and cell migration are required for epithelial wound healing. The proliferation of corneal epithelial cells in the process of migration during wound healing is inhibited until the wound is covered.[39] The apparent discrepancy between the increased proliferation capacity of corneal epithelial cells and the delayed corneal wound healing in GK rats may reflect differential regulation of the proliferation and migration of these cells during wound healing. For example, whereas epidermal growth factor stimulates the proliferation and migration of corneal epithelial cells, fibronectin stimulates only cell migration.[40,41] However, EGF and fibronectin stimulate the healing of corneal epithelial defects in vivo.

Our immunohistochemical results on the localization of Cx43, K14, and Ki-67 indicate that the corneal epithelium of GK rats has an immature phenotype characterized by a double layer of basal-like cells. This phenotype might reflect the increased proliferation of corneal epithelial basal cells in GK rats. This increased proliferation may thus result in upward migration of the basal cells before they have matured into wing cells. It does not appear that the increased production of basal cells in GK rats results in increased lateral migration of these cells during wound healing.

The proliferation of epithelial cells is thought to be influenced by the local glucose concentrations surrounding the cornea, such as those in tear fluid,[42,43] aqueous humor,[44,45] and basement membrane. The proliferation of human corneal epithelial cells has thus been shown to be increased[15] or decreased[16] by exposure to high glucose concentrations in vitro. The proliferation of corneal epithelial cells, as revealed by the uptake of [^{3}H]-thymidine, was found to be increased in rats with streptozotocin-induced diabetes, and the corneal epithelium of these animals appeared immature.[18] The results of this previous study are thus consistent with our present observations in the GK rat. In contrast, the proliferation of corneal epithelial cells was found to be decreased in the KKAy mouse model of type 2 diabetes.[17] However, KKAy mice develop obesity and hyperlipidemia in addition to hyperglycemia, possibly explaining this difference in findings.

GK rats manifest characteristics similar to those of diabetic complications of the cornea in humans, including delayed epithelial wound healing,[4,5] lowered corneal sensation,[46,47] and reduced tear secretion.[48,49] Many animal models have been studied for investigation into diabetic complications, including genetic models such as the KKAy mouse,[17,50] the db/db mouse,[51] and the Otsuka Long-Evans Tokushima Fatty (OLETF) rat.[52,53] However, these models develop obesity or hyperlipidemia and hyperglycemia, which complicates the attribution of pathologic changes specifically to hyperglycemia. In contrast, the GK rat develops hyperglycemia during embryonic development but does not develop obesity or hyperlipidemia. Our present results thus suggest that the GK rat is a suitable animal model for studies into the pathogenesis of diabetic keratopathy.

References

1. Yach D, Alberti G. *Screening for Type 2 Diabetes*. Geneva: World Health Organization; 2003.
2. Brodrick JD. Corneal problems after retinal and vitreous surgery. *Trans Ophthalmol Soc UK*. 1975;95:138–141.
3. Foulks GN, Thoft RA, Perry HD, Tolentino FI. Factors related to corneal epithelial complications after closed vitrectomy in diabetics. *Arch Ophthalmol*. 1979;97:1076–1078.
4. Fukushi S, Merola LO, Tanaka M, Datiles M, Kinoshita JH. Reepithelialization of denuded corneas in diabetic rats. *Exp Eye Res*. 1980;31:611–621.
5. Schultz RO, van Horn DL, Peters MA, Klewin KM, Schutten WH. Diabetic keratopathy. *Am J Ophthalmol Soc*. 1981;79:180–199.
6. Taylor HR, Kimsey RA. Corneal epithelial basement membrane changes in diabetes. *Invest Ophthalmol Vis Sci*. 1981;20:548–553.
7. Friend J, Ishii Y, Thoft RA. Corneal epithelial changes in diabetic rats. *Ophthalmic Res*. 1982;14:269–278.
8. Azar DT, Spurr-Michaud SJ, Tisdale AS, Gipson IK. Decreased penetration of anchoring fibrils into the diabetic stroma: a morphometric analysis. *Arch Ophthalmol*. 1989;107:1520–1523.
9. Sato N, Nakamura M, Chikama T, Nishida T. Abnormal deposition of laminin and type IV collagen at corneal epithelial basement membrane during wound healing in diabetic rats. *Jpn J Ophthalmol*. 1999;43:343–347.
10. Kabosova A, Kramerov AA, Aoki AM, Murphy G, Zieske JD, Ljubimov AV. Human diabetic corneas preserve wound healing, basement membrane, integrin and MMP-10 differences from normal corneas in organ culture. *Exp Eye Res*. 2003;77:211–217.
11. Ljubimov AV, Huang Z, Huang GH, et al. Human corneal epithelial basement membrane and integrin alterations in diabetes and diabetic retinopathy. *J Histochem Cytochem*. 1998;46:1033–1041.
12. Morishige N, Chikama T, Nishida T. Abnormal scattering detected by confocal biomicroscopy at the corneal epithelial basement membrane of subjects with type II diabetes. *Diabetologia*. 2001; 44:340–345.
13. McDermott AM, Xiao TL, Kern TS, Murphy CJ. Non-enzymatic glycation in corneas from normal and diabetic donors and its effects on epithelial cell attachment in vitro. *Optometry*. 2003;74: 443–452.
14. Kaji Y, Usui T, Oshika T, et al. Advanced glycation end products in diabetic corneas. *Invest Ophthalmol Vis Sci*. 2000;41:362–368.
15. McDermott AM, Kern TS, Murphy CJ. The effect of elevated extracellular glucose on migration, adhesion and proliferation of SV40 transformed human corneal epithelial cells. *Curr Eye Res*. 1998;17:924–932.
16. Fujita H, Morita I, Takase H, Ohno-Matsui K, Mochizuki M. Prolonged exposure to high glucose impaired cellular behavior of normal human corneal epithelial cells. *Curr Eye Res*. 2003;27:197–203.

17. Watanabe H, Katakami C, Miyata S, Negi A. Corneal disorders in KKAy mouse: a type 2 diabetes model. *Jpn J Ophthalmol*. 2002; 46:130–139.
18. Yamamoto N, Katakami C, Yamamoto M. Proliferation of corneal epithelial cells in diabetic rats (in Japanese). *Nippon Ganka Gakkai Zasshi*. 1998;102:475–480.
19. Thoft RA, Friend J. The X, Y, Z hypothesis of corneal epithelial maintenance. *Invest Ophthalmol Vis Sci*. 1983;24:1442–1443.
20. Scermer A, Galvin S, Sun TT. Differentiation-related expression of a major 64K corneal keratin in vivo and in culture suggests limbal location of corneal epithelial stem cells. *J Cell Biol*. 1986;103:49–62.
21. Sun TT, Shih C, Green H. Keratin cytoskeletons in epithelial cells of internal organs. *Proc Natl Acad Sci USA*. 1979;76:2813–2817.
22. Dong Y, Roos M, Gruijters T. Differential expression of two gap junction proteins in corneal epithelium. *Eur J Cell Biol*. 1994;64: 95–100.
23. Laux-Fenton WT, Donaldson PJ, Kistler J, Green CR. Connexin expression patterns in the rat cornea. *Cornea*. 2003;22:457–464.
24. Suzuki K, Tanaka T, Enoki M, Nishida T. Coordinated reassembly of the basement membrane and junctional proteins during corneal epithelial wound healing. *Invest Ophthalmol Vis Sci*. 2000;41: 2495–2500.
25. Matic M, Petrov IN, Rosenfeld T, Wolosin JM. Alterations in connexin expression and cell communication in healing corneal epithelium. *Invest Ophthalmol Vis Sci*. 1997;38:600–609.
26. Suzuki K, Saito J, Yanai R, et al. Cell-matrix and cell-cell interactions during corneal epithelial wound healing. *Prog Retin Eye Res*. 2003;22:113–133.
27. Nakamura M, Nishida T, Ofuji K, Reid TW, Mannis MJ, Murphy CJ. Synergistic effect of substance P with epidermal growth factor on epithelial migration in rabbit cornea. *Exp Eye Res*. 1997;65:321–329.
28. Cameron JD, Hagen ST, Waterfield RR, Furcht LT. Effects of matrix proteins on rabbit corneal epithelial cell adhesion and migration. *Curr Eye Res*. 1988;7:293–301.
29. Tervo K, Tervo T, van Setten GB, Tarkkanen A, Virtanen I. Demonstration of tenascin-like immunoreactivity in rabbit corneal wounds. *Acta Ophthalmol (Copenh)*. 1989;67:347–350.
30. Goto Y, Suzuki K, Ono T, Sasaki M, Toyota T. Development of diabetes in the non-obese NIDDM rat (GK rat). *Adv Exp Med Biol*. 1988;246:29–31.
31. Goto Y. What do spontaneously diabetic animals suggest (in Japanese)? *Nippon Naika Gakkai Zasshi*. 1988;77:1177–1185.
32. Janssen U, Riley SG, Vassiliadou A, Floege J, Phillips AO. Hypertension superimposed on type II diabetes in Goto Kakizaki rats induces progressive nephropathy. *Kidney Int*. 2003;63:2162–2170.
33. Sato N, Komatsu K, Kurumatani H. Late onset of diabetic nephropathy in spontaneously diabetic GK rats. *Am J Nephrol*. 2003;23: 334–342.
34. Suzuki K, Yen-Chung H, Toyota T, Goto Y, Hirata Y, Okada K. The significance of nerve sugar levels for the peripheral nerve impairment of spontaneously diabetic GK (Goto-Kakizaki) rats. *Diabetes Res*. 1990;14:21–25.
35. Miyamoto K, Ogura Y, Nishiwaki H, et al. Evaluation of retinal microcirculatory alterations in the Goto-Kakizaki rat: a spontaneous model of non-insulin-dependent diabetes. *Invest Ophthalmol Vis Sci*. 1996;37:898–905.
36. Carmo A, Cunha-Vaz JG, Carvalho AP, Lopes MC. Nitric oxide synthase activity in retinas from non-insulin-dependent diabetic Goto-Kakizaki rats: correlation with blood-retinal barrier permeability. *Nitric Oxide*. 2000;4:590–596.
37. Sone H, Kawakami Y, Okuda Y, et al. Ocular vascular endothelial growth factor levels in diabetic rats are elevated before observable retinal proliferative changes. *Diabetologia*. 1997;40:726–730.
38. Akimoto Y, Kawakami H, Yamamoto K, Munetomo E, Hida T, Hirano H. Elevated expression of O-GlcNAc-modified proteins and O-GlcNAc transferase in corneas of diabetic Goto-Kakizaki rats. *Invest Ophthalmol Vis Sci*. 2003;44:3802–3809.
39. Trinkaus-Randall V, Edelhauser HF, Leibowitz HM, et al. Corneal structure and function. In: Leibowitz HM, Waring GO, eds. *Corneal Disorders*. 2nd ed. Philadelphia: WB Saunders;1998:2–31.
40. Murakami J, Morimoto K, Nishida T, et al. Movement of corneal epithelium of rats in situ observed by time-lapse cinematography. In: Shimizu K, ed. *Current Aspects in Ophthalmology*. Vol. 1. Amsterdam: Elsevier 1992;315–319.
41. Watanabe K, Nakagawa S, Nishida T. Stimulatory effects of fibronectin and EGF on migration of corneal epithelial cells. *Invest Ophthalmol Vis Sci*. 1987;28:205–211.
42. Gasset AR, Braverman LE, Fleming MC, Arky RA, Alter BR. Tear glucose detection of hyperglycemia. *Am J Ophthalmol*. 1968:65; 414–420.
43. Tapaszto I. Pathophysiology of human tears. *Int Ophthalmol Clin*. 1973;13:119–147.
44. Kashintseva LT. Intraocular fluid metabolism in patients with diabetes mellitus (in Russian). *Oftalmol Zh*. 1965;20:448–451.
45. Bito LZ. The physiology and pathophysiology of intraocular fluids. *Exp Eye Res*. 1977;25(suppl):273–289.
46. Daubs JG. Diabetes screening with corneal aesthesiometer. *Am J Optom Physiol Opt*. 1975;52:31–35.
47. Nielsen NV. Corneal sensitivity and vibratory perception in diabetes mellitus. *Acta Ophthalmol (Copenh)*. 1978;56:406–411.
48. Andersen J, Baun O, Aamand HE. Tear secretion in juvenile diabetics with and without autonomic neuropathy. *Acta Ophthalmol (Copenh)*. 1985;63:93–96.
49. Saito J, Enoki M, Hara M, Morishige N, Chikama T, Nishida T. Correlation of corneal sensation, but not of basal reflex tear secretion, with stage of diabetic retinopathy. *Cornea*. 2003;22:15–18.
50. Iwatsuka H, Shino A, Suzuoki Z. General survey of diabetic features of yellow KK mice. *Endocrinol Jpn*. 1970;17:23–35.
51. Hummel KP, Dickie MM, Coleman DL. Diabetes, a new mutation in the mouse. *Science*. 1966;153:1127–1128.
52. Kawano K, Hirashima T, Mori S, Saitoh Y, Kurosumi M, Natori T. Spontaneous long-term hyperglycemic rat with diabetic complications: Otsuka Long-Evans Tokushima Fatty (OLETF) strain. *Diabetes*. 1992;41:1422–1428.
53. Saika S, Shimezaki M, Ohkawa K, et al. Ultrastructural examination of corneal epithelium of spontaneously obese, hyperglycemic rats. *Curr Eye Res*. 1998;17:1049–1057.